Mechanics of Materials 12 (1991) 267–278
Elsevier

Edge effect of a carbon fiber meeting a surface

C.C. Li and E.S. Folias

Department of Mechanical Engineering, University of Utah, Salt Lake City, UT 84112, USA

Received 26 October 1990; revised version received 25 June 1991

This paper investigates the free edge effect on the stress field of a carbon fiber, which is embedded into an epoxy matrix. The fiber is assumed to possess cylindrical symmetry and to be transversely isotropic. The matrix is assumed to be of an isotropic material. The stress field is induced by a uniform tension applied on the matrix at points far away from the fiber surface.

The displacement and stress fields are explicitly derived and a stress singularity is shown to prevail. The singularity strength is shown to be a function of the material constants of the fiber as well as those of the matrix. Finally, the displacement and stress profiles are plotted as a function of the angle ϕ which is measured from the free surface.

1. Introduction

Quite often in engineering practice, structures are composed of two elastic materials with different properties which are bonded together over some surface. Such type of problem has been investigated from a 2D point of view by many researchers and the results can be found in the literature. For example, Knein (1927) considered the plane strain problem of an orthogonal elastic wedge bonded to a rigid base. Rongved (1955) investigated the problem of two bonded elastic half-spaces subjected to a concentrated force in the interior. Subsequently, Williams (1959) studied the stress field around a fault or a crack in dissimilar media. The work was then generalized by Rice and Sih (1965) to also include arbitrary angles.

It was not until 1968 that Bogy (1968) considered the general problem of two bonded quarter-planes of dissimilar isotropic, elastic materials subjected to arbitrary boundary tractions. The problem was solved by an application of the Mellin transform in conjunction with the Airy stress function. The same author (1971) extended his work to also include dissimilar wedges of arbitrary angles. Shortly thereafter, Hein and Erdogan (1971), using the same method of solution, independently reproduced the results by Bogy. Finally, Westmann (1975) studied the case of a wedge of an arbitrary angle which was bonded along a finite length to a half-space. His analysis showed the presence of two singularities close to each other. Thus, elimination of the first singular term does not lead to a bounded stress field since the second singularity is still present.

Based on 3D consideration, Luk and Keer (1979) investigated the stress field in an elastic half-space containing a partially embedded axially loaded, rigid cylindrical rod. The problem was formulated in terms of Hankel integral transforms and was finally cast into a system of coupled singular integral equations the solution of which was sought numerically. The authors were able, however, to extract in the limit from the integral equations the characteristic equation governing the singular behavior at the intersection of the free surface and that of the rigid inclusion. Their result was in agreement with that obtained by Williams (1952) for a right-angle corner with fixed–free boundary conditions.

Haritos and Keer (1979) investigated the stress field in a half-space containing an embedded rigid block under conditions of plane strain. The problem was formulated by cleverly superimposing the solutions to the problem of horizontal and vertical line inclusions beneath an elastic half-space. By isolating the pertinent terms, the authors were able to extract directly from the integral equations the order of the stress

singularity at both corners. Both results are in agreement with the Williams solution. Moreover, the authors point out the importance of the second singularity to the results of the load transfer problems.

With the advancement of composites and their extensive use in the aerospace industry, problems for the determination of the stress and displacement fields around inclusions have drawn considerable attention. For instance, Goodier (1933) investigated the disturbing effect of small spherical and cylindrical inclusions on an otherwise uniform stress distribution plate. Numerical results were presented for flaws, perfectly bonded rigid inclusions and slag globules cases. Hardiman (1952) used the complex variable method to treat the elliptic inclusion problem, he was the first to find that a uniform applied load at infinity induces a constant state of stress within an elliptic inclusion. The work was later generalized by Sendeckyj (1970) to include the solutions of the elastic curvilinear inclusions problems. It was not until 1979 that Tirosh, Katz and Lifschuetz (1979) studied the stress interaction of a single fiber, embedded in an elastic matrix, with a micro-crack situated near the interface. They found that the radial tensile stress component σ_{rr} is higher than the tangential component $\sigma_{\theta\theta}$, and the location r at which the maximum stress takes place is not on the interface but at a small distance ahead, depending on the Poisson's ratio of the matrix. Dundurs (1989) noticed that the stresses in a body that contains rigid inclusions and is subjected to a specified surface traction depend on the Poisson's ratio of the material. If the Poisson's ratio is set equal to $+1$ for plane strain, or $+\infty$ for plane stress, the rigid inclusions become cavities for elastic constants within the physical range.

In the area of multiple or periodical inclusions problems, Adams and Doner (1967) obtained a 2D numerical solution by a systematic overrelaxation procedure for a plate containing a rectangular array of inclusions embedded in an elastic matrix and subjected to a uniform normal transverse stress at infinity. At the same time, Goree (1967) presented a solution for the stress and displacement distributions in an infinite elastic matrix containing two perfectly bonded rigid cylindrical inclusions of different radii. Subsequently, Haener and Ashbaugh (1967) used the displacement potentials method to express the stress distributions in a unidirectional multiple fibers composite plate under external and residual loads. Marloff and Daniel (1969) used a standard stress–freezing technique to determine the 3D stress distribution in the matrix of a unidirectional composite plate subjected to matrix shrinkage and normal transverse load. Based on Sendeckyj's previous work, Yu and Sendeckyj (1974) extended their study by means of the Schwarz alternating method to the case of an infinite elastic matrix containing a random number of elastic inclusions. Moreover, Adams and Crane (1984) studied a microscopic region of a unidirectional composite plate by the finite element micromechanical analysis using a generalized plane strain formulation. Finally, Keer, Dundurs and Kiattikomol (1973) studied the phenomena of the separation of a smooth circular inclusion from a matrix which is subjected to a uniform load. Using finite integral transforms, the problem of finding the extension of separation and the contact pressure is reduced to the solution of a Fredholm integral equation with a weakly singular Kernel.

Recently, Folias (1989) examined the local stress field in the neighborhood where a fiber embedded into an epoxy matrix meets a free surface. In this analysis, Folias assumed the fiber and the matrix to be isotropic but of different material constants. The analysis showed that the stress field in this vicinity to be singular. Moreover, the 3D analysis showed that for the case of a cylindrical inclusion, the order of the singularity strength is precisely that which was reported by Bogy (1968) based on 2D consideration. In the present paper the analysis is extended to also include a transversely isotropic fiber, e.g. carbon fiber, and the explicit 3D displacement and stress fields are recovered.

2. Formulation of the problem

Consider the equilibrium of a cylindrical carbon fiber of radius a which is embedded into a homogeneous, isotropic and linear elastic matrix that occupies the space $|x| < \infty$, $|y| < \infty$ and $|z| \leqslant h$.

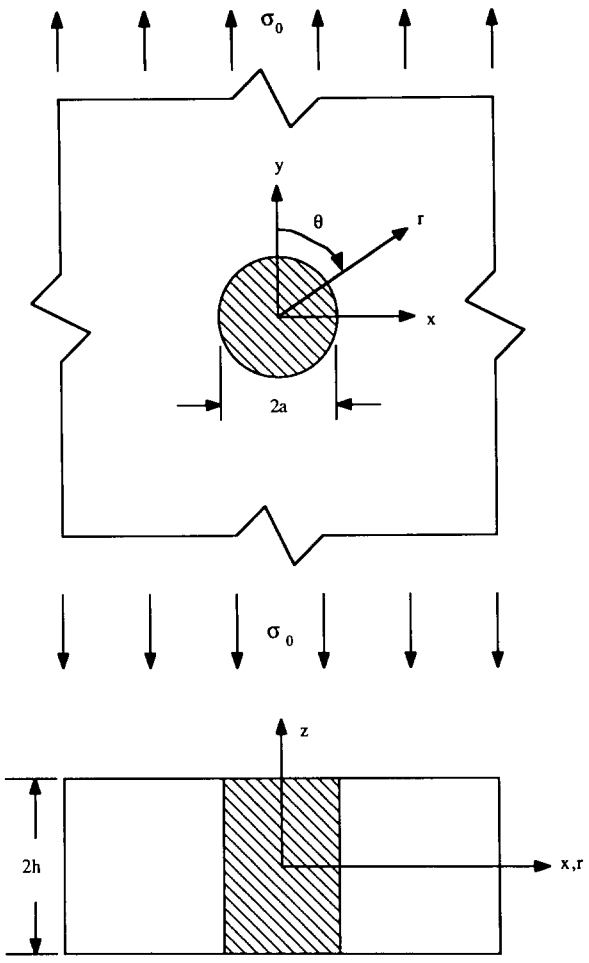

Fig. 1. Infinite plate of arbitrary thickness with cylindrical inclusion.

The fiber is assumed to be of a transversely isotropic material with different material properties than those of the matrix. Moreover, the axis of the fiber is assumed to intersect the bounding plane $z = \pm h$ perpendicularly and the matrix to be subjected to a uniform tensile load σ_0 in the direction of the y-axis and parallel to the xy-plane (see Fig. 1). Perfect bonding at the interface is assumed to prevail.

In the absence of body forces, the equilibrium equations, in terms of the stresses σ_{ij}, are:

$$\frac{\partial \sigma_{rr}^{(m)}}{\partial r} + \frac{1}{r}\frac{\partial \tau_{r\theta}^{(m)}}{\partial \theta} + \frac{\partial \tau_{rz}^{(m)}}{\partial z} + \frac{\sigma_{rr}^{(m)} - \sigma_{\theta\theta}^{(m)}}{r} = 0, \tag{1}$$

$$\frac{\partial \tau_{r\theta}^{(m)}}{\partial r} + \frac{1}{r}\frac{\partial \sigma_{\theta\theta}^{(m)}}{\partial \theta} + \frac{\partial \tau_{\theta z}^{(m)}}{\partial z} + \frac{2\tau_{r\theta}^{(m)}}{r} = 0, \tag{2}$$

$$\frac{\partial \tau_{rz}^{(m)}}{\partial r} + \frac{1}{r}\frac{\partial \tau_{\theta z}^{(m)}}{\partial \theta} + \frac{\partial \sigma_{zz}^{(m)}}{\partial z} + \frac{\tau_{rz}^{(m)}}{r} = 0, \tag{3}$$

where superscript $m = 1$ represents the material of the matrix and $m = 2$ represents the material of the fiber.

The stress–strain relations for a transversely isotropic [1], as well as an isotropic, material are given by the constitutive relations

$$\begin{bmatrix} \sigma_{rr}^{(m)} \\ \sigma_{\theta\theta}^{(m)} \\ \sigma_{zz}^{(m)} \\ \tau_{\theta z}^{(m)} \\ \tau_{zr}^{(m)} \\ \tau_{r\theta}^{(m)} \end{bmatrix} = \begin{bmatrix} C_{11}^{(m)} & C_{12}^{(m)} & C_{13}^{(m)} & 0 & 0 & 0 \\ C_{12}^{(m)} & C_{11}^{(m)} & C_{13}^{(m)} & 0 & 0 & 0 \\ C_{13}^{(m)} & C_{13}^{(m)} & C_{33}^{(m)} & 0 & 0 & 0 \\ 0 & 0 & 0 & C_{44}^{(m)} & 0 & 0 \\ 0 & 0 & 0 & 0 & C_{44}^{(m)} & 0 \\ 0 & 0 & 0 & 0 & 0 & \frac{1}{2}\left(C_{11}^{(m)} - C_{12}^{(m)}\right) \end{bmatrix} \begin{bmatrix} \epsilon_{rr}^{(m)} \\ \epsilon_{\theta\theta}^{(m)} \\ \epsilon_{zz}^{(m)} \\ \gamma_{\theta z}^{(m)} \\ \gamma_{zr}^{(m)} \\ \gamma_{r\theta}^{(m)} \end{bmatrix}, \tag{4}$$

where the $C_{ij}^{(m)}$ represent the respective material constants.

As to boundary conditions, we require that (i) the stresses on the planes $z = \pm h$ must vanish and (ii) that the displacements and stresses of the two materials must match at the interface, i.e. at $r = a$.

3. Method of solution

The primary objective of this analysis is to derive an asymptotic solution which is valid in the immediate vicinity of the corner points, i.e. the points where the interface meets the free surface of the matrix. Thus following the same method of solution as that of Folias (1989), one may write the equilibrium equations (1)–(3) in terms of the displacements $u_{ij}^{(m)}$ as [2]

$$C_{11}^{(m)} \frac{\partial^2 u_r^{(m)}}{\partial (r-a)^2} + \left(C_{13}^{(m)} + C_{44}^{(m)}\right) \frac{\partial^2 w^{(m)}}{\partial (r-a)\, \partial z} + C_{44}^{(m)} \frac{\partial^2 u_r^{(m)}}{\partial z^2} = 0, \tag{5}$$

$$\tfrac{1}{2}\left(C_{11}^{(m)} - C_{12}^{(m)}\right) \frac{\partial^2 u_\theta^{(m)}}{\partial (r-a)^2} + C_{44}^{(m)} \frac{\partial^2 u_\theta^{(m)}}{\partial z^2} = 0, \tag{6}$$

$$C_{44}^{(m)} \frac{\partial^2 w^{(m)}}{\partial (r-a)^2} + \left(C_{44}^{(m)} + C_{13}^{(m)}\right) \frac{\partial^2 u_r^{(m)}}{\partial (r-a)\, \partial z} + C_{33}^{(m)} \frac{\partial^2 w^{(m)}}{\partial z^2} = 0. \tag{7}$$

It is interesting to note that the stress field, at the vicinity of the fiber interface, leads to two coupled equations (5) and (7) for the displacements $u_r^{(m)}$ and $w^{(m)}$ and an additional equation (6) for the displacement $u_\theta^{(m)}$.

Without going into the mathematical details, by direct substitution, one can show that the following displacement field satisfies the governing equations (5)–(7):

$$u_r^{(m)} = -\left(C_{13}^{(m)} + C_{44}^{(m)}\right) \frac{\partial^2 H^{(m)}}{\partial (r-a)\, \partial z}, \tag{8}$$

$$w^{(m)} = \left(C_{11}^{(m)} \frac{\partial^2}{\partial (r-a)^2} + C_{44}^{(m)} \frac{\partial^2}{\partial z^2} \right) H^{(m)}, \tag{9}$$

$$u_\theta^{(m)} = \tilde{H}^{(m)}, \tag{10}$$

[1] The material of the fiber is assumed to possess a cylindrical symmetry.

[2] In writing the following equations, we assumed that $r - a \ll a$.

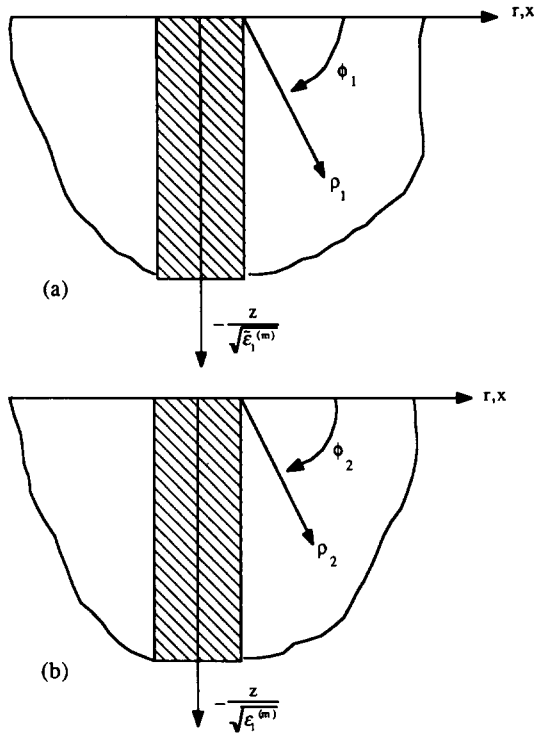

Fig. 2. Definition of two local coordinate systems (a) and (b) at the corner.

where the pseudo-harmonic functions $H^{(m)}$ and $\tilde{H}^{(m)}$ satisfy the equations

$$\left(\frac{\partial^2}{\partial(r-a)^2}+\epsilon_1^{(m)}\frac{\partial^2}{\partial z^2}\right)\left(\frac{\partial^{(m)}}{\partial(r-a)^2}+\epsilon_2^{(m)}\frac{\partial^2}{\partial z^2}\right)H^{(m)}=0 \tag{11}$$

and

$$\left(\frac{\partial^2}{\partial(r-a)^2}+\tilde{\epsilon}_1^{(m)}\frac{\partial^2}{\partial z^2}\right)\tilde{H}^{(m)}=0 \tag{12}$$

with

$$\epsilon_{1,2}^{(m)}=\tfrac{1}{2}c_m\pm\tfrac{1}{2}\sqrt{c_m^2-4d_m}\,, \tag{13}$$

$$\tilde{\epsilon}_1^{(m)}=\frac{2C_{44}^{(m)}}{\left(C_{11}^{(m)}-C_{12}^{(m)}\right)}, \tag{14}$$

$$d_m=\frac{C_{33}^{(m)}}{C_{11}^{(m)}}, \tag{15}$$

$$c_m=\frac{C_{33}^{(m)}}{C_{44}^{(m)}}-\frac{C_{13}^{(m)^2}}{C_{11}^{(m)}C_{44}^{(m)}}-\frac{2C_{13}^{(m)}}{C_{11}^{(m)}}. \tag{16}$$

It is found convenient at this stage to introduce the local coordinate system (see Fig. 2),

$$r-a=\rho\cos\phi, \tag{17}$$

$$h-z=\rho\sin\phi \tag{18}$$

and to adopt the following definitions:

$$\rho_1 = \rho\sqrt{\cos^2\phi + \frac{\sin^2\phi}{\tilde{\epsilon}_1^{(m)}}}\,, \tag{19}$$

$$\rho_2 = \rho\sqrt{\cos^2\phi + \frac{\sin^2\phi}{\epsilon_1^{(m)}}}\,, \tag{20}$$

$$\phi_1 = \tan^{-1}\left(\frac{\tan\phi}{\sqrt{\tilde{\epsilon}_1^{(m)}}}\right), \tag{21}$$

$$\phi_2 = \tan^{-1}\left(\frac{\tan\phi}{\sqrt{\epsilon_1^{(m)}}}\right), \tag{22}$$

in view of which, one may now construct asymptotic solutions for the functions $H^{(m)}$ and $\tilde{H}^{(m)}$ in ascending powers of ρ, i.e.

$$H^{(m)} = \rho_2^{\alpha+1}\cos(\beta\theta)\Big\{A_2^{(m)}\cos\big[(\alpha+1)\phi_2\big] + B_2^{(m)}\sin\big[(\alpha+1)\phi_2\big] + \frac{1}{(\alpha+1)}\int_0^{\phi_2}\psi^{(m)}(\zeta)\sin\big[(\alpha+1)(\phi_2-\zeta)\big]\,d\zeta\Big\} + O\big(\rho_2^{\alpha+2}\big) \tag{23}$$

and

$$\tilde{H}^{(m)} = \rho_1^{\alpha+1}\cos(\beta\theta)\big\{A_1^{(m)}\cos\big[(\alpha+1)\phi_1\big] + B_1^{(m)}\sin\big[(\alpha+1)\phi_1\big]\big\} + O\big(\rho_1^{\alpha+2}\big), \tag{24}$$

where

$$\psi^{(m)}(\xi) = \left\{A_3^{(m)}\cos\left[(\alpha-1)\tan^{-1}\left(\sqrt{\frac{\epsilon_1^{(m)}}{\epsilon_2^{(m)}}}\tan\xi\right)\right] + B_3^{(m)}\sin\left[(\alpha-1)\tan^{-1}\left(\sqrt{\frac{\epsilon_1^{(m)}}{\epsilon_2^{(m)}}}\tan\xi\right)\right]\right\}\left(\frac{1+\left(\epsilon_1^{(m)}/\epsilon_2^{(m)}\right)\tan^2\xi}{1+\tan^2\xi}\right)^{\alpha/2-1} \tag{25}$$

and α, $A_1^{(m)}$, $B_1^{(m)}$, $A_2^{(m)}$, $B_2^{(m)}$, $A_3^{(m)}$ and $B_3^{(m)}$ are unknown constants to be determined from the following boundary conditions:

$$\text{at } \phi = 0: \qquad \sigma_{zz}^{(1)} = \tau_{rz}^{(1)} = \tau_{\theta z}^{(1)} = 0, \tag{26}$$

$$\text{at } \phi = \pi: \qquad \sigma_{zz}^{(2)} = \tau_{rz}^{(2)} = \tau_{\theta z}^{(2)} = 0, \tag{27}$$

$$\text{at } \phi = \pi/2: \qquad u_r^{(1)} = u_r^{(2)}, \quad u_\theta^{(1)} = u_\theta^{(2)}, \quad w^{(1)} = w^{(2)}, \tag{28}$$

$$\sigma_{rr}^{(1)} = \sigma_{rr}^{(2)}, \quad \tau_{r\theta}^{(1)} = \tau_{r\theta}^{(2)}, \quad \tau_{rz}^{(1)} = \tau_{rz}^{(2)}. \tag{29}$$

Substituting the previously constructed displacement field into the boundary conditions (26)–(29), we arrive at a system of twelve algebraic equations, the determinant of which must vanish. This latter condition leads to a transcendental equation for the characteristic value α.

Without going into the mathematical details, these characteristic values α may easily be determined with the aid of a computer. Although the transcendental equation has an infinite number of real roots,

only those values which lie in the interval $1 < \alpha < 2$ are of practical interest. Furthermore, in this interval there are no complex roots present. In general α depends on the respective material properties of the matrix as well as of the fiber.

The displacement and stress fields may now be computed in terms of one unknown constant which in turn is to be determined from the loading conditions far away from the fiber–matrix interface. Without going into the mathematical details, the explicit displacement and stress fields are found to be:

(i) displacement field:

$$u_r^{(m)} = \frac{1}{\sqrt{\epsilon_1^{(m)}}}\left(C_{13}^{(m)} + C_{44}^{(m)}\right)\alpha(\alpha+1)\rho_2^{\alpha-1}\cos(\beta\theta)$$
$$\times\left\{-A_2^{(m)}\sin[(\alpha-1)\phi_2] + B_2^{(m)}\cos[(\alpha-1)\phi_2]\right.$$
$$\left. + \frac{1}{(\alpha+1)}\int_0^{\phi_2}\psi^{(m)}(\zeta)\cos[(\alpha-1)\phi_2 - (\alpha+1)\zeta]\,d\zeta - \frac{\cos\phi_2\sin\phi_2}{\alpha(\alpha+1)}\psi^{(m)}(\phi_2)\right\}$$
$$+ O(\rho_2^{\alpha}), \tag{30}$$

$$w^{(m)} = \alpha(\alpha+1)\rho_2^{\alpha-1}\cos(\beta\theta)$$
$$\times\left\{\left(C_{11}^{(m)} - \frac{C_{44}^{(m)}}{\epsilon_1^{(m)}}\right)\left\{A_2^{(m)}\cos[(\alpha-1)\phi_2] + B_2^{(m)}\sin[(\alpha-1)\phi_2]\right.\right.$$
$$\left. + \frac{1}{(\alpha+1)}\int_0^{\phi_2}\psi^{(m)}(\zeta)\sin[(\alpha-1)\phi_2 - (\alpha+1)\zeta]\,d\zeta\right\}$$
$$\left. + \left[C_{11}^{(m)}\frac{\sin^2\phi_2}{\alpha(\alpha+1)} + \frac{C_{44}^{(m)}}{\epsilon_1^{(m)}}\frac{\cos^2\phi_2}{\alpha(\alpha+1)}\right]\psi^{(m)}(\phi_2)\right\} + O(\rho_2^{\alpha}), \tag{31}$$

$$u_\theta^{(m)} = \alpha(\alpha+1)\rho_1^{\alpha-1}\cos(\beta\theta)\left\{A_1^{(m)}\cos[(\alpha-1)\phi_1] + B_1^{(m)}\sin[(\alpha-1)\phi_1]\right\} + O(\rho_1^{\alpha}); \tag{32}$$

(ii) stress field:

$$\sigma_{rr}^{(m)} = -\frac{1}{\sqrt{\epsilon_1^{(m)}}}C_{44}^{(m)}(\alpha-1)\alpha(\alpha+1)\rho_2^{\alpha-2}\cos(\beta\theta)$$
$$\times\left\{\left(C_{11}^{(m)} + \frac{C_{13}^{(m)}}{\epsilon_1^{(m)}}\right)\left\{A_2^{(m)}\sin[(\alpha-2)\phi_2] - B_2^{(m)}\cos[(\alpha-2)\phi_2]\right.\right.$$
$$\left. - \frac{1}{(\alpha+1)}\int_0^{\phi_2}\psi^{(m)}(\zeta)\cos[(\alpha-2)\phi_2 - (\alpha+1)\zeta]\,d\zeta\right\}$$
$$+ \left[\left(C_{11}^{(m)} + \frac{C_{13}^{(m)}}{\epsilon_1^{(m)}}\right)\frac{\sin 2\phi_2\cos\phi_2}{\alpha(\alpha+1)} - C_{11}^{(m)}\frac{\sin^3\phi_2}{\alpha(\alpha+1)} + \frac{C_{13}^{(m)}}{\epsilon_1^{(m)}}\frac{\cos^2\phi_2\sin\phi_2}{\alpha(\alpha+1)}\right]\psi^{(m)}(\phi_2)$$
$$\left. + \left[-C_{11}^{(m)}\frac{\sin^2\phi_2\cos\phi_2}{(\alpha-1)\alpha(\alpha+1)} + \frac{C_{13}^{(m)}}{\epsilon_1^{(m)}}\frac{\cos^3\phi_2}{(\alpha-1)\alpha(\alpha+1)}\right]\psi^{(m)\prime}(\phi_2)\right\} + O(\rho_2^{\alpha-1}), \tag{33}$$

$$\sigma_{\theta\theta}^{(m)} = -\frac{1}{\sqrt{\epsilon_1^{(m)}}}(\alpha-1)\alpha(\alpha+1)\rho_2^{\alpha-2}\cos(\beta\theta)$$
$$\times\left\{\left[C_{12}^{(m)}\left(C_{13}^{(m)}+C_{44}^{(m)}\right)-C_{13}^{(m)}\left(C_{11}^{(m)}-\frac{C_{44}^{(m)}}{\epsilon_1^{(m)}}\right)\right]\right.$$
$$\times\left\{A_2^{(m)}\sin\left[(\alpha-2)\phi_2\right]-B_2^{(m)}\cos\left[(\alpha-2)\phi_2\right]\right.$$
$$\left.-\frac{1}{(\alpha+1)}\int_0^{\phi_2}\psi^{(m)}(\zeta)\cos\left[(\alpha-2)\phi_2-(\alpha+1)\zeta\right]\,d\zeta\right\}$$
$$+\left\{\left[C_{12}^{(m)}\left(C_{13}^{(m)}+C_{44}^{(m)}\right)-C_{13}^{(m)}\left(C_{11}^{(m)}-\frac{C_{44}^{(m)}}{\epsilon_1^{(m)}}\right)\right]\frac{\sin 2\phi_2\cos\phi_2}{\alpha(\alpha+1)}\right.$$
$$+\left[-C_{12}^{(m)}\left(C_{13}^{(m)}+C_{44}^{(m)}\right)+C_{13}^{(m)}C_{11}^{(m)}\right]\frac{\sin^3\phi_2}{\alpha(\alpha+1)}$$
$$\left.+\frac{C_{13}^{(m)}C_{44}^{(m)}}{\epsilon_1^{(m)}}\frac{\cos^2\phi_2\sin\phi_2}{\alpha(\alpha+1)}\right\}\psi^{(m)}(\phi_2)$$
$$+\left\{\left[-C_{12}^{(m)}\left(C_{13}^{(m)}+C_{44}^{(m)}\right)+C_{13}^{(m)}C_{11}^{(m)}\right]\frac{\sin^2\phi_2\cos\phi_2}{(\alpha-1)\alpha(\alpha+1)}\right.$$
$$\left.\left.+\frac{C_{13}^{(m)}C_{44}^{(m)}}{\epsilon_1^{(m)}}\frac{\cos^3\phi_2}{(\alpha-1)\alpha(\alpha+1)}\right\}\psi^{(m)'}(\phi_2)\right\}+O\left(\rho_2^{\alpha-1}\right), \tag{34}$$

$$\sigma_{zz}^{(m)} = -\frac{1}{\sqrt{\epsilon_1^{(m)}}}(\alpha-1)\alpha(\alpha+1)\rho_2^{\alpha-2}\cos(\beta\theta)$$
$$\times\left\{\left[C_{13}^{(m)}\left(C_{13}^{(m)}+C_{44}^{(m)}\right)-C_{33}^{(m)}\left(C_{11}^{(m)}-\frac{C_{44}^{(m)}}{\epsilon_1^{(m)}}\right)\right]\right.$$
$$\times\left\{A_2^{(m)}\sin\left[(\alpha-2)\phi_2\right]-B_2^{(m)}\cos\left[(\alpha-2)\phi_2\right]\right.$$
$$\left.-\frac{1}{(\alpha+1)}\int_0^{\phi_2}\psi^{(m)}(\zeta)\cos\left[(\alpha-2)\phi_2-(\alpha+1)\zeta\right]d\zeta\right\}$$
$$+\left\{\left[C_{13}^{(m)}\left(C_{13}^{(m)}+C_{44}^{(m)}\right)-C_{33}^{(m)}\left(C_{11}^{(m)}-\frac{C_{44}^{(m)}}{\epsilon_1^{(m)}}\right)\right]\frac{\sin 2\phi_2\cos\phi_2}{\alpha(\alpha+1)}\right.$$
$$+\left[-C_{13}^{(m)}\left(C_{13}^{(m)}+C_{44}^{(m)}\right)+C_{33}^{(m)}C_{11}^{(m)}\right]\frac{\sin^3\phi_2}{\alpha(\alpha+1)}$$
$$\left.+\frac{C_{33}^{(m)}C_{44}^{(m)}}{\epsilon_1^{(m)}}\frac{\cos^2\phi_2\sin\phi_2}{\alpha(\alpha+1)}\right\}\psi^{(m)}(\phi_2)$$
$$+\left\{\left[-C_{13}^{(m)}\left(C_{13}^{(m)}+C_{44}^{(m)}\right)+C_{33}^{(m)}C_{11}^{(m)}\right]\frac{\sin^2\phi_2\cos\phi_2}{(\alpha-1)\alpha(\alpha+1)}\right.$$
$$\left.\left.+\frac{C_{33}^{(m)}C_{44}^{(m)}}{\epsilon_1^{(m)}}\frac{\cos^3\phi_2}{(\alpha-1)\alpha(\alpha+1)}\right\}\psi^{(m)'}(\phi_2)\right\}+O\left(\rho_2^{\alpha-1}\right), \tag{35}$$

$$\tau_{rz}^{(m)} = C_{44}^{(m)}(\alpha-1)\alpha(\alpha+1)\rho_2^{\alpha-2}\cos(\beta\theta)$$
$$\times\left\{\left(C_{11}^{(m)}+\frac{C_{13}^{(m)}}{\epsilon_1^{(m)}}\right)\left\{A_2^{(m)}\cos[(\alpha-2)\phi_2]+B_2^{(m)}\sin[(\alpha-2)\phi_2]\right.\right.$$
$$\left.+\frac{1}{(\alpha+1)}\int_0^{\phi_2}\psi^{(m)}(\zeta)\sin[(\alpha-2)\phi_2-(\alpha+1)\zeta]\,d\zeta\right\}$$
$$+\left[\left(C_{11}^{(m)}+\frac{C_{13}^{(m)}}{\epsilon_1^{(m)}}\right)\frac{\sin 2\phi_2\sin\phi_2}{\alpha(\alpha+1)}-\frac{C_{13}^{(m)}}{\epsilon_1^{(m)}}\frac{\cos^3\phi_2}{\alpha(\alpha+1)}+C_{11}^{(m)}\frac{\sin^2\phi_2\cos\phi_2}{\alpha(\alpha+1)}\right]\psi^{(m)}(\phi_2)$$
$$\left.+\left[-C_{11}^{(m)}\frac{\sin^3\phi_2}{(\alpha-1)\alpha(\alpha+1)}+\frac{C_{13}^{(m)}}{\epsilon_1^{(m)}}\frac{\cos^2\phi_2\sin\phi_2}{(\alpha-1)\alpha(\alpha+1)}\right]\psi^{(m)\prime}(\phi_2)\right\}+O(\rho_2^{\alpha-1}), \tag{36}$$

$$\tau_{\theta z}^{(m)} = -\frac{1}{\sqrt{\epsilon_1^{(m)}}}C_{44}^{(m)}(\alpha-1)\alpha(\alpha+1)\rho_1^{\alpha-2}\cos(\beta\theta)$$
$$\times\left\{-A_1^{(m)}\sin[(\alpha-1)\phi_1]+B_1^{(m)}\cos[(\alpha-1)\phi_1]\right\}+O(\rho_1^{\alpha-1}), \tag{37}$$

$$\tau_{r\theta}^{(m)} = \tfrac{1}{2}\left(C_{11}^{(m)}-C_{12}^{(m)}\right)(\alpha-1)\alpha(\alpha+1)\rho_1^{\alpha-2}\cos(\beta\theta)$$
$$\times\left\{A_1^{(m)}\cos[(\alpha-1)\phi_1]+B_1^{(m)}\sin[(\alpha-1)\phi_1]\right\}+O(\rho_1^{\alpha-1}). \tag{38}$$

4. Discussion

As a practical matter, two different types of fibers embedded into an epoxy matrix were considered, a carbon fiber and a glass fiber defined by the elastic properties given in Table 1.

Omitting the long and tedious numerical details, the characteristic values of α were found to be $\alpha = 1.693$ and $\alpha = 1.737$, respectively [3]. The analysis suggests that the presence of a carbon fiber induces a slightly higher singular stress field than that of a glass fiber and consequently is more prone to failure. Moreover, in the limit, one recovers precisely the corresponding isotropic solution derived by Folias (1989). In Figs. 3–6, the behaviors of the local displacement and stress fields as a function of angular

[3] It may be noted that a second real root exists within this interval, however it leads to a slightly weaker stress singularity (see Westmann, 1975).

Table 1
The material properties for carbon fiber, glass fiber and epoxy matrix

Carbon fiber	Glass fiber	Epoxy matrix
$C_{11} = 20.40$ MPa	$C_{11} = 99.19$ MPa	$C_{11} = 6.62$ MPa
$C_{12} = 9.40$ MPa	$C_{12} = 27.69$ MPa	$C_{12} = 3.41$ MPa
$C_{13} = 10.50$ MPa		
$C_{33} = 240.00$ MPa		
$C_{44} = 24.00$ MPa		

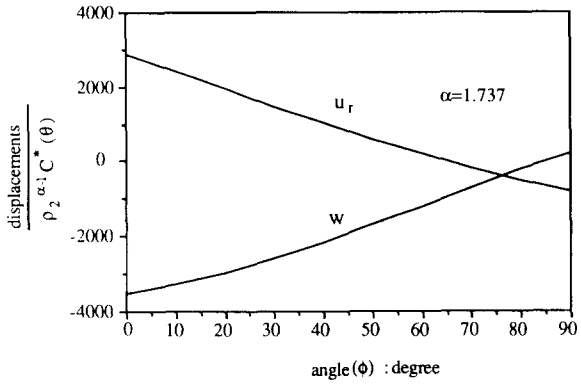

Fig. 3. Displacements versus ϕ for isotropic case.

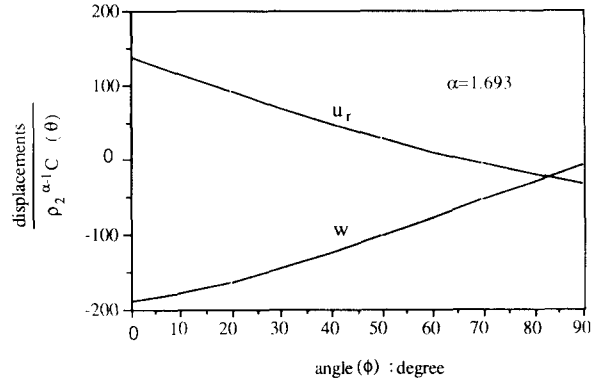

Fig. 4. Displacements versus ϕ for transversely isotropic case.

distribution ϕ are depicted for both fibers considered above. The reader may note that for simplicity we have adopted the definition

$$C(\theta) = A_2^{(2)}\alpha(\alpha + 1)\cos(\beta\theta), \tag{39}$$

which in the limit, as the material constants

$$C_{ij} \to C_{ij_{\text{isotropic}}}, \tag{40}$$

the function

$$C(\theta) \to C^*(\theta). \tag{41}$$

It is noteworthy that, although the displacement and stress profiles corresponding to the two different fibers are very similar, their respective magnitudes are different. Similar trends are also expected to prevail at locations further away from the free surface. Finally, it remains for us to relate the unknown constant $A_2^{(2)}$ to the applied load far away from the vicinity of the fiber. This matter is presently under investigation, and the results will be reported in a future paper where we will also take into account other effects such as stresses due to a temperature mismatch, mechanical loads along and perpendicular to the fiber axis, and a

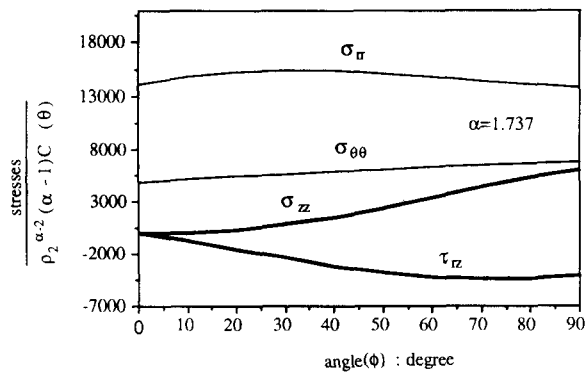

Fig. 5. Stresses versus ϕ for isotropic case.

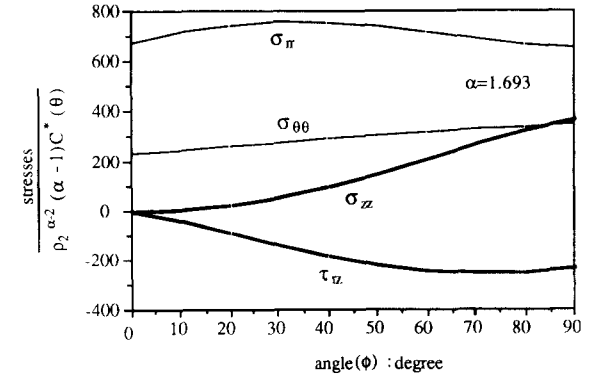

Fig. 6. Stresses versus ϕ for transversely isotropic case.

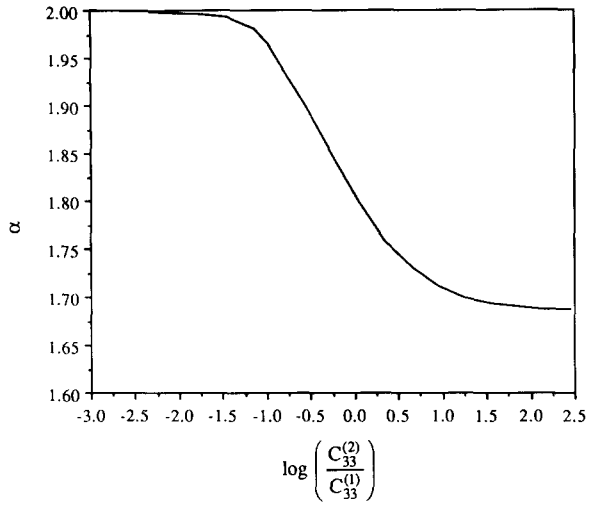

Fig. 7. The value of the characteristic constant α versus $\log(C_{33}^{(2)}/C_{33}^{(1)})$.

correction factor to account for the presence of a periodic array of fibers embedded into a matrix. Finally, the variation of the exponent α as a function of the material ratio $C_{33}^{(2)}/C_{33}^{(1)}$ is given by Fig. 7.

Acknowledgement

This work was supported in part by the Air Force Office of Scientific Research Grant No. AFOSR-90-0351. The authors wish to thank Lt. Col. G. Haritos for this support and for various discussions.

References

Adams, D.F. and D.R. Doner (1967), Transverse normal loading of a unidirectional composite, *J. Composite Mater. 1*, 152.

Adams, D.F. and D.A. Crane (1984), Combined loading micro-mechanical analysis of a unidirectional composite, *Composites 15*, 181.

Bogy, D.B. (1968), Edge-bonded dissimilar orthogonal elastic wedges under normal and shear loading, *J. Appl. Mech. 35*, 460.

Bogy, D.B. (1971), Two edge-bonded elastic wedges of different materials and wedge angles under surface tractions, *J. Appl. Mech. 38*, 377.

Dundurs, J. (1989). Cavities vis-à-vis rigid inclusions and some related general results in plane elasticity, *J. Appl. Mech. 56*, 786.

Folias, E.S. (1989), On the stress singularities at the intersection of a cylindrical inclusion with the free surface of a plate, *Int. J. Fracture 39*, 25.

Goodier, J.N. (1933), Concentration of stress around spherical and cylindrical inclusions and flaws, *The American Society of Mechanical Engineers 55*, 39.

Goree, J.G. (1967), In plane loading in an elastic matrix containing two cylindrical inclusions, *J. Composite Mater. 1*, 404.

Haener, J. and N. Ashbaugh (1967), Three-dimensional stress distribution in a unidirectional composite, *J. Composite Mater. 1*, 54.

Hardiman, N.J. (1952), Elliptic elastic inclusion in an infinite elastic plate, *Q. J. Appl. Math. Mech. 7*, 226.

Haritos, G.K. and L.M. Keer (1979), Stress analysis for an elastic half space containing an embedded rigid block, *Int. J. Solids Struct. 16*, 19.

Hein, V.L. and F. Erdogan (1971), Stress singularities in a two-material wedge, *Int. J. Fracture 7*, 317.

Keer, L.M., J. Dundurs and K. Kiattikomol (1973), Separation of a smooth circular inclusion from a matrix, *Int. J. Eng. Sci. 11*, 1221.

Knein, M. (1927), *Zur Theorie der Druckversuchs*, Abhandlungen der Aerodynamishe Inst. u.d. Technishe Hochschule, Aachen, Germany.

Luk, V.K. and L.M. Keer (1979), Stress analysis for an elastic half space containing an axially-loaded rigid cylindrical rod, *Int. J. Solids Struct. 15*, 805.

Marloff, R.H. and I.M. Daniel (1969), Three-dimensional photoelastic analysis of a fiber-reinforced composite model, *Exp. Mech. 9*, 156.

Rice, J.R. and G.C. Sih (1965), Plane problems of cracks in dissimilar media, *J. Appl. Mech. E32*, 418.

Rongved, L. (1955), Force interior to one of two jointed semi-infinite solids, Second Midwestern Conference on Solid Mechanics 1.

Sendeckyj, G.P. (1970), Elastic inclusion problems in plane elastostatics, *Int. J. Solids Struct. 6*, 1535.

Tirosh, J., Katz, E. and G. Lifschuetz (1979), The role of fibrous reinforcements well bonded or parially debonded on the transverse strength of composite materials, *Eng. Fracture Mech. 12*, 267.

Westmann, R.A. (1975), Geometrical effects in adhesive joints, *Int. J. Eng. Sci. 13*, 369.

Williams, M.L. (1952), Stress singularities resulting from various boundary conditions in angular corners of plates in extension, *J. Appl. Mech. 19*, 526.

Williams, M.L. (1959), *Bull. Seismo. Soc. Am.* 199.

Yu, I.W. and G.P. Sendeckyj (1974), Multiple circular inclusion problems in plane elastostatics, *J. Appl. Mech. 41*, 215.